Development of a Universal Colorimetric Indicator for G-Quadruplex Structures by the Fusion of Thiazole Orange and Isaindigotone Skeleton

ARTICLE *in* ANALYTICAL CHEMISTRY · JULY 2012

Impact Factor: 5.64 · DOI: 10.1021/ac300207r · Source: PubMed

analytical chemistry

Letter

pubs.acs.org/ac

Development of a Universal Colorimetric Indicator for G-Quadruplex Structures by the Fusion of Thiazole Orange and Isaindigotone Skeleton

Jin-Wu Yan, Wen-Jie Ye, Shuo-Bin Chen, Wei-Bin Wu, Jin-Qiang Hou, Tian-Miao Ou, Jia-Heng Tan,* Ding Li, Lian-Quan Gu, and Zhi-Shu Huang*

School of Pharmaceutical Sciences, Sun Yat-sen University, Guangzhou 510006, China

Supporting Information

ABSTRACT: The rapid and convenient method for identification of all kinds of G-quadruplex is highly desirable. In the present study, a novel colorimetric indicator for a vast variety of G-quadruplex was designed and synthesized on the basis of thiazole orange and isaindigotone skeleton. Its distinct color change enables label-free visual detection of G-quadruplexes, which is due to the disassembly of dye H-aggregates to monomers. This specific detection of G-quadruplex arises from its end-stacking interaction with G-quartet. On the basis of this universal indicator, a facile approach for large-scale identification of G-quadruplex was developed.

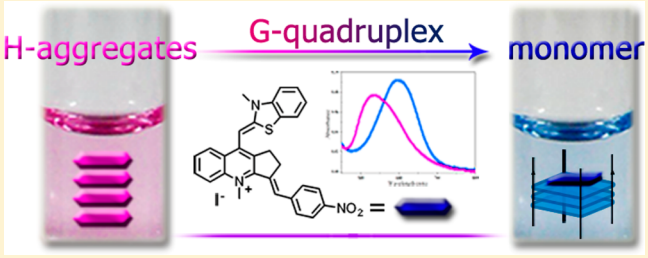

The selective and facile detection of nucleic acids is important for basic research and many applied fields, such as clinical diagnosis and gene therapy.[1−3] G-Quadruplexes are unique secondary structures formed by G-rich nucleic acid sequences in many pivotal genomic regions, such as telomeric DNA, promoter region of some oncogenes and RNA sequences.[4−7] G-Quadruplex structures are receiving great attention as uncovering their important biological functions and applications in supramolecular chemistry and nanotechnology.[8−14] Due to their significance in both biology and supramolecular chemistry, the detection of G-quadruplex is very important. In recent years, much effort has been made to exploit the sensors including organic probes, metal complexes, and nanoparticles, for the detection of G-quadruplexes.[15−19] With the advantage of easy manipulation and low cost, the colorimetric organic dyes with clear and rapid visual readouts for G-quadruplexes are extremely attractive. Recently, some cyanine dyes have been developed to achieve colorimetric detection of certain kinds of intramolecular G-quadruplex DNAs,[20−22] but these methods are not suitable for broad-spectrum identification of G-quadruplex. As we know, widespread putative G-quadruplex-forming sequences exist, which exhibit significant structural polymorphism depending on different sequences and conditions, including parallel, antiparallel, and hybrid types. Thus, it is highly desirable to develop a universal approach for the rapid, facile, and instrument-free detection of all kinds of G-quadruplexes. To the best of our knowledge, the application of organic dyes to colorimetric detection of a vast variety of G-quadruplexes has not been reported. In the present study, we designed and developed a universal colorimetric dye, which could be applied for label-free large-scale detection of a vast variety of G-quadruplexes.

A promising strategy for universal detection of a variety of G-quadruplexes is to design a probe interacting through end-stacking with G-quartet that is the common binding site for all types of G-quadruplexes. Thiazole orange (TO, Figure 1), a widely used probe for nucleic acids,[23−27] is composed of a quinoline ring linked to a benzothiazole ring through a methine bridge. TO can stack on the G-quartet and has been used in G-quadruplex fluorescent intercalator displacement assay to study the interaction between G-quadruplex and its ligands.[28,29] In addition, TO tends to aggregate in aqueous medium due to its

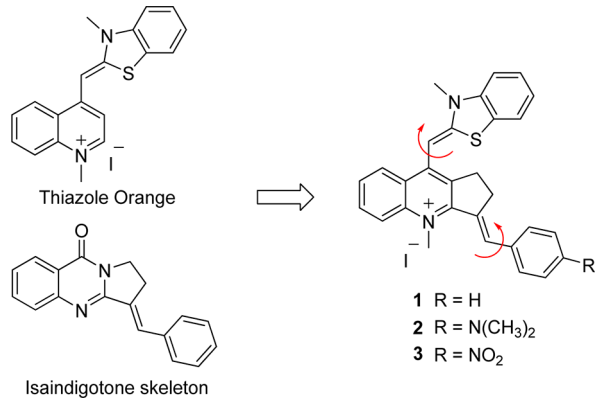

Figure 1. Structures of thiazole orange, isaindigotone skeleton, and the fusion dyes.

Received: January 19, 2012
Accepted: July 17, 2012
Published: July 17, 2012

intermolecular van der Waals forces and transforms to its monomers in the presence of G-quadruplexes, being accompanied with an indistinctive shift of their absorption peaks (Figure S1, Supporting Information). Accordingly, the supramolecular assembly and end-stacking feature of TO could be used in our design strategy. The application of TO for the detection of G-quadruplexes is limited by its drawback of poor selectivity for G-quadruplex from other forms of DNAs; therefore, it is necessary to improve the selectivity of this dye molecule. Isaindigotone (Figure 1) is a naturally occurring alkaloid, which is commonly used in traditional Chinese medicine. Isaindigotone derivatives developed in our lab have shown excellent binding affinity and selectivity for G-quadruplexes.[30,31] Our previous studies have demonstrated that their selectivity for G-quadruplexes can be partially attributed to their adaptive styryl moiety and their five-member aliphatic ring.

Inspired by these studies on isaindigotone derivatives with high selectivity for G-quadruplex and the self-assembly of TO with end-stacking on G-quartet, we attempted to assemble isaindigotone and TO in a fusion scaffold (Figure 1), aiming to optimize its photophysical property and selectivity for G-quadruplex through its expanded π-conjugate aromatic system and the effect of its tunable R group. The expanded aromatic system with a positive charge ensures the appropriate end-stacking interaction between the dyes and the G-quartet. The five-member aliphatic ring and the free rotation of the single bond may not only make this adaptive aromatic structure to stack well on the G-quartet but also diminish its interaction with the duplex DNAs.

Three desired dyes with different R groups (Figure 1) were prepared (Scheme 1), and their assembly properties in different

Scheme 1. Synthetic Route for Compounds 1−3[a]

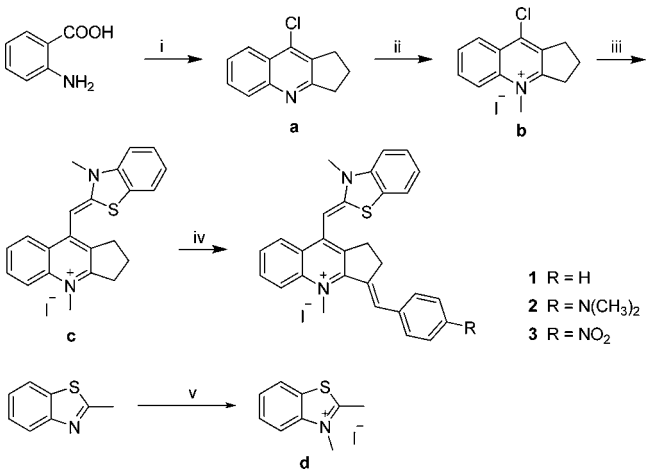

[a]Reagents and conditions: (i) cyclopentanone, $POCl_3$, reflux; (ii) CH_3I, tetramethylene sulfone, 50 °C; (iii) compound **d**, sodium bicarbonate, methanol, room temperature then reflux; (iv) aromatic aldehyde, piperidine, *n*-butanol, 80 °C; (v) CH_3I, ethanol, 80 °C.

solvents were investigated using UV−vis absorption spectra. As expected, all these three compounds exist mainly as a monomeric state in organic solvents, and the blue-shifted absorption band of aggregation could be observed in buffer, which is assigned to H-aggregates (Figure S1, Supporting Information). H-aggregates of dye molecules occur in the case of a face-to-face stacking of the monomers and a parallel alignment of the transition dipoles perpendicular to the axis of stacking.[32−34] A blue-shifted absorption band is typically observed for H-aggregates. The UV−vis spectrum of compound **3** showed that the absorption peak of H-aggregates (535 nm) blue-shifted 63 nm as compared to its monomeric species (Table S3, Supporting Information), which is the largest shift among these three dyes. To clarify the unique assembly properties of compound **3** and make a further comparison among all three compounds and TO, the molecular geometry optimization and calculation were carried out using HF/6-311++G(d,p) basis set by Gaussian 03 program. The results showed that the dipole moments of compound **3** were much larger than other compounds, and the molecular electrostatic potential (ESP) charges were also evidently influenced by the electron-withdrawing nitro group (Figure S2 and Table S4, Supporting Information), and those of compounds **1** and **2** and TO were close to each other. Such calculation results were in good agreement with the experimental data. The large dipole moment of compound **3** generated a strong intermolecular dipole−dipole coupling interaction and the efficient formation of compact aggregates at higher dye loading, consequently giving the largest blue shift; thus, we selected **3** for further studies.

The interactions of **3** with G-quadruplex were studied using UV−vis spectroscopic titrations. As shown in Figure 2A, **3** exhibited a predominant H-aggregation band around 535 nm in buffer; upon titration with G-quadruplex-forming oligonucleotide (pu27), dramatic changes of the absorption peaks were observed. The peak around 535 nm gradually decreased with addition of G-quadruplex and eventually led to the appearance of a new peak around 600 nm assigned to its monomeric state, which is consistent with the disassembly of the H-aggregates of **3**. Interestingly, the red shift for the disassembly of the H-aggregates of **3** to its monomers gave rise to a clear and visible color change from purplish red to blue (Figure 3A). Meanwhile, we applied **3** for the detection of G-quadruplexes with varying sequences and conformations, including parallel and antiparallel, intramolecular and intermolecular structures. The results showed that all these G-quadruplexes could be detected colorimetrically through incubation with **3** (Figures S3 and S4, Supporting Information). Thus, **3** could be used as a rapid and facile indicator for a variety of G-quadruplexes.

Besides, the selectivity of **3** in detection of G-quadruplexes over single and duplex DNAs was studied with UV spectra. Figure 2B showed the absorbance enhancement at 600 nm against the ratio of [DNA]/[**3**]. Obviously, G-quadruplexes, including pu27, c-kit1, HTG21, and tetramer could remarkably increase the absorbance at 600 nm. In contrast, non-quadruplexes, including single strands (dA21 and dT21), linear duplex CT-DNA (calf thymus DNA), and self-complementary duplex strand (ds15) could hardly affect the aggregation state of **3** under the same condition, with only slight decrease of the absorbance (Figures S5 and S6, Supporting Information). Thus, G-quadruplexes could be easily detected and differentiated from other forms of DNA with just the naked eye (Figure 3A). Moreover, the application of **3** for the detection of G-quadruplex RNA was also investigated, and it was found that **3** could also differentiate G-quadruplex RNA from single/duplex strand RNAs and total RNA in cell lysate (Figures 3B and S7, Supporting Information). The above results indicated that **3** could be used for label-free visual detection of a variety of G-quadruplexes with high specificity.

dx.doi.org/10.1021/ac300207r | *Anal. Chem.* 2012, 84, 6288−6292

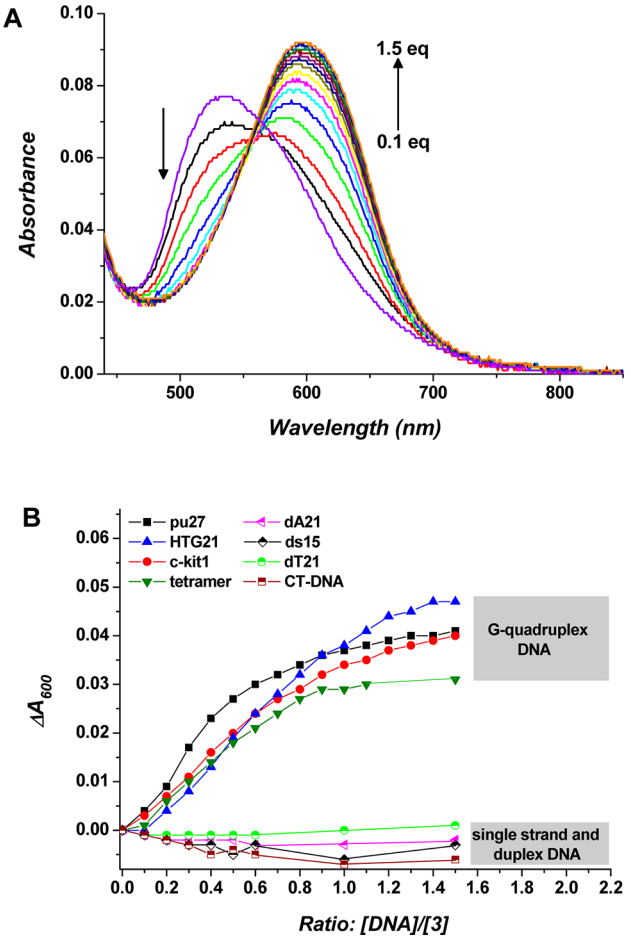

Figure 2. (A) UV−vis spectra for titration of 5 μM **3** stepwise to G-quadruplex-forming oligonucleotide (pu27). Conditions: [**3**] = 5 μM; in 10 mM Tris−HCl buffer, 60 mM KCl, pH 7.4. The spectra were recorded at 4 min intervals. (B) The absorbance enhancement of 5 μM **3** at 600 nm against the ratio of [DNA]/[**3**].

In order to examine whether the color change of **3** was due to its interactions with G-quadruplex secondary structures or simply just G-rich sequences, we mixed HTG21 and its complementary sequence in a ratio of 1:1 to form a G-rich duplex structure.[35] In contrast with the HTG21 G-quadruplex, the G-rich duplex structure could not induce clear color change (Figure 3C), which demonstrated that **3** indeed interacts with G-quadruplex secondary structures instead of simple G-rich sequences to generate color change.

To study the practical usage of **3** in detecting G-quadruplexes, we used **3** in testing two newly reported G-quadruplexes: hras-1, STAT3, and their mutant sequences.[36,37] As we expected, the wild-type G-quadruplexes hras-1 and STAT3 could be easily detected and differentiated from their mutant sequences with the naked eye (Figure 3D), which further indicated that this method could be developed as an easy and reliable approach for rapid detection of G-quadruplexes.

On the basis of the above universal colorimetric detection of a variety of G-quadruplexes with **3**, a rapid and convenient method for large-scale identification of G-quadruplexes was developed. The absorbance at 535 and 600 nm represents the content of H-aggregates and monomers, respectively. The specific interaction of **3** with G-quadruplexes can disassemble the H-aggregates; as shown in the spectra, the absorbance at

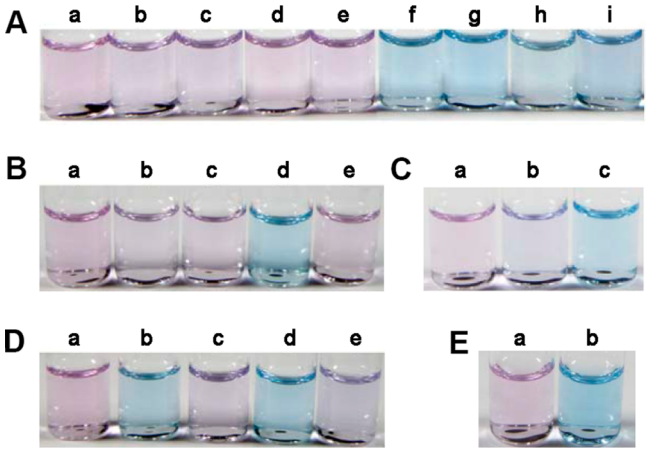

Figure 3. (A) Photograph of 10 μM **3** H-aggregates (a) and 10 μM **3** with 20 μM dA21 (b); dT21 (c); CT-DNA (d); ds15 (e); pu27 (f); c-kit1 (g); HTG21 (h); tetramer (i). (B) Photograph of 10 μM **3** H-aggregates (a) and 10 μM **3** with 20 μM ssRNA (b); dsRNA (c); G-quadruplex RNA (d); total RNA in cell lysate (e). (C) Photograph of 10 μM **3** H-aggregates (a) and 10 μM **3** with a 20 μM 1:1 mixture of HTG21 and its complementary sequence (b); HTG21 only (c). (D) Photograph of 10 μM **3** H-aggregates (a) and 10 μM **3** with 20 μM STAT3 (b); STAT3-mut (c); hras-1 (d); hras-1-mut (e). (E) Photograph of 10 μM **3** H-aggregates (a) and 10 μM **3** with 20 μM HT-6 (b).

600 nm was significantly enhanced and that at 535 nm was decreased. Thus, the value of A_{600}/A_{535} could reflect the ability of DNA to disassemble the H-aggregates. On the basis of the above buffer conditions, the concentration and ratio of compound **3** and DNA was optimized as follows (Figure S8A,B, Supporting Information): the samples containing 10 μM **3** and 10 μM DNA with varying secondary structures were dissolved in 150 μL of 10 mM Tris−HCl buffer containing 60 mM K^+, which were then added to 96-well plates. After incubation for 4 min at 25 °C, the absorbance at 535 and 600 nm for the samples was determined using a 96-well microplate reader. As shown in Figure 4, the values of A_{600}/A_{535} were above 1.4 for all types of G-quadruplexes, while the values were below 0.9 for nonquadruplexes. Therefore, it is possible and reasonable to judge the secondary structures of DNA based on

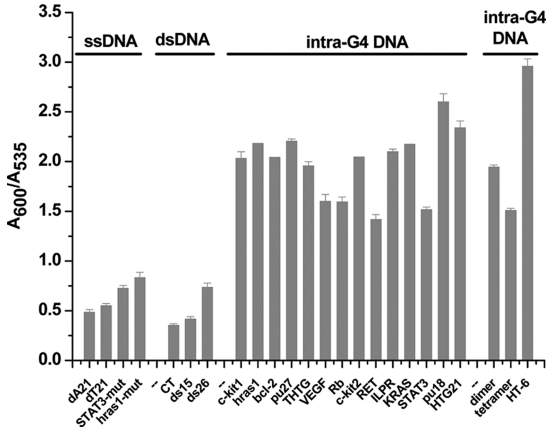

Figure 4. Distribution for the values of the A_{600}/A_{535} for all the tested oligonucleotides. Conditions: [**3**] = 10 μM, [DNA] = 10 μM, in 10 mM Tris−HCl buffer, 60 mM KCl, pH 7.4. The absorbance of the samples was determined using a 96-well microplate reader.

dx.doi.org/10.1021/ac300207r | *Anal. Chem.* 2012, 84, 6288−6292

the values of A_{600}/A_{535}. To obtain the optimal discrepancy of A_{600}/A_{535} between G-quadruplexes and nonG-quadruplexes, we further screened the buffer conditions, including pH, concentration of K^+, and different types of buffer solutions. We found that the values of A_{600}/A_{535} were only slightly influenced by the buffer conditions (Figure S8C,E, Supporting Information), which indicated that this facile method is reliable and widely applicable.

To further clarify and rationalize the application of **3** for the specific detection of G-quadruplexes, FRET-melting assay, surface plasma resonance (SPR) and nuclear magnetic resonance (NMR) studies were performed. The FRET results (Figure S9 and Table S5, Supporting Information) showed that **3** could stabilize G-quadruplexes without effect on T_m value of the hairpin duplex DNA (F10T), suggesting its excellent selectivity to G-quadruplexes. In addition, the binding affinity and selectivity for G-quadruplexes of **3** and TO were assessed by SPR experiments. The binding constants of **3** to G-quadruplexes fell into a range (K_D, 0.429−0.735 μM), while no specific interaction between **3** and single/duplex strands was observed (Figure S10 and Table S6, Supporting Information). The binding affinity indicated that **3** exhibited high selectivity for G-quadruplexes over single and duplex strands, which was much better than TO. In the NMR study, the tetramolecular parallel G-quadruplex HT-6 $[d(T_2AG_3)]_4$ derived from human telomeric DNA was used as a template, which could also induce the color change of **3** (Figure 3E).[38] An NMR titration experiment showed that most ^{1}H NMR signals exhibited progressive shifts and line broadening at increasing concentration of **3**, which were slightly more obvious for imino proton signals of G4 (Figure S11, Supporting Information). Furthermore, with increasing concentration of **3**, the imino proton signals of A3H2, A3H8, and G4H8 exhibited significant line broadening. These results and previous NMR studies suggested that **3** preferred to stack on the G4 G-quartet plane.[39,40]

On the basis of these results, we believe that the external-stacking mode should be the main reason for the successful application of **3** in the detection of a vast variety of G-quadruplexes, because G-quartet is the common building block of all kinds of G-quadruplexes. The binding affinity between **3** and G-quadruplex is higher than the intermolecular affinity of H-aggregates of **3**, and consequently, **3** is attracted to the G-quartet in the form of monomer. In contrast, there is no such specific and strong interaction between **3** and nonquadruplex structures; thus, **3** is likely to remain in the form of H-aggregates.

CONCLUSIONS

In summary, three novel dyes were rationally designed and synthesized, and compound **3** can be used for visual detection and differentiation of G-quadruplexes from single and duplex DNA structures. The transformation for H-aggregates of **3** to its monomer induced by its end-stacking interaction with G-quartet gave rise to a distinct color change, which make it become a rapid and facile detection method for G-quadruplexes. On the basis of this universal colorimetric indicator, a simple and reliable approach for large-scale identification of G-quadruplexes was developed, which should have promising application in the field of G-quadruplex research.

EXPERIMENTAL SECTION

Chemicals. All oligonucleotides were purchased from Invitrogen (Shanghai, China) and Sangon (Shanghai, China). Calf thymus DNA (CT-DNA) was purchased from Sigma-Aldrich (Singapore). All the oligonucleotides were dissolved in Tris−HCl buffer (10 mM, containing 60 mM KCl, pH 7.4), and the concentration of oligonucleotides was determined from their absorbance at 260 nm using NanoDrop 1000 (Thermo). The samples were prepared through heating at 95 °C for 10 min followed with slow cooling to room temperature.

UV−Visible and Fluorescence Measurements. UV−vis spectra were obtained with a Shimadzu 2450 Spectrophotometer. The labeled oligonucleotides were used as the FRET probes. Fluorescence melting curves were determined with a Roche LightCycler 2 real-time PCR machine, using a total reaction volume of 20 mL, with 0.2 μM of labeled oligonucleotide in 10 mM Tris−HCl buffer, pH 7.4, 60 mM KCl. Fluorescence readings with excitation at 470 nm and detection at 530 nm were taken at intervals of 1 °C over the range of 37−99 °C, with a constant temperature being maintained for 30 s prior to each reading to ensure a stable value. The melting of the G-quadruplex was monitored alone or in the presence of **3**. Final analysis of the data was carried out using Origin 8.0 (OriginLab Corp.). Emission of 6-carboxyfluorescein was normalized between 0 and 1, and $T_{1/2}$ was defined as the temperature for which the normalized emission is 0.5. $\Delta T_{1/2}$ values were derived from the mean of three experimental data.

SPR Assays. SPR measurements were performed on a ProteOn XPR36 Protein Interaction Array system (Bio-Rad Laboratories, Hercules, CA) using a Neutravidin-coated GLH sensor chip. Biotinylated oligonucleotides (HTG: $(GTTAGG)_5$; c-myc: $ACGTACGTGGGG-(AGGGTGGGG)_2AAGGTGGGG$; c-kit1: AGG-GAGGGCGCTGGGAGGAGGG; single strand: $(AGTTAG)_5$; hairpin duplex DNA: TTCGCGCGCGTTTTCGCGCGCG) were attached to a streptavidin-coated sensor chip. In a typical experiment, biotinylated DNA was folded in filtered and degassed running buffer (50 mM Tris−HCl, pH 7.2, 100 mM KCl). The DNA samples were then captured (∼1000 RU) in flow cells 1−3, leaving the fourth flow cell as a blank. Ligand solutions were prepared with running buffer through serial dilutions of stock solution. Five concentrations were injected simultaneously at a flow rate of 50 mL·min^{-1} for 400 s of association phase, followed with 400 s of dissociation phase at 25 °C. The GLH sensor chip was regenerated with short injection of 50 mM NaOH between consecutive measurements. The final graphs were obtained by subtracting blank sensorgrams from quadruplex and duplex sensorgrams.

NMR Study. NMR experiments were performed on a Bruker 600 MHz spectrometer. All of the titration experiments were carried out at 25 °C in a 90% H_2O/10% D_2O solution containing 150 mM KCl and 25 mM potassium phosphate buffer (pH 7.2). The oligonucleotide HT-6 was purified using HPLC, and the concentration of intermolecular G-quadruplex $[d(TTAGGG)]_4$ was 0.5 mM for the NMR measurements.

ASSOCIATED CONTENT

Supporting Information

Synthetic procedures and characterization data, including ^{1}H NMR, ^{13}C NMR, NOESY NMR, HRMS, and HPLC spectra for compounds (**1**−**3**); photophysical properties of compounds

dx.doi.org/10.1021/ac300207r | Anal. Chem. 2012, 84, 6288−6292

(**1**−**3**); UV−vis spectra and photographs of **3** with different nucleic acid motifs; stabilization of DNA G-quadruplexes and duplex by **3** determined by FRET melting assays; binding constants (K_D) of **3** for its binding to G-quadruplexes measured with SPR assays; NMR study on binding of **3** with the tetramolecular parallel G-quadruplex. This material is available free of charge via the Internet at http://pubs.acs.org.

AUTHOR INFORMATION

Corresponding Author

*E-mail: ceshzs@mail.sysu.edu.cn (Z.-S.H.); tanjiah@mail.sysu.edu.cn (J.-H.T.). Fax: 8620-39943056 (Z.-S.H.). Phone: 8620-39943056 (Z.-S.H.); 8620-39943053 (J.-H.T.).

Notes

The authors declare no competing financial interest.

ACKNOWLEDGMENTS

This work was supported by National Natural Science Foundation of China (Nos. 90813011, 21172272, 81001400) and the International S&T Cooperation Program of China (No. 2010DFA34630).

REFERENCES

(1) Rosi, N. L.; Giljohann, D. A.; Thaxton, C. S.; Lytton-Jean, A. K.; Han, M. S.; Mirkin, C. A. *Science* **2006**, *312*, 1027−1030.
(2) Fu, R.; Li, T.; Park, H. G. *Chem. Commun.* **2009**, *39*, 5838−5840.
(3) Robertson, K. L.; Thach, D. C. *Anal. Biochem.* **2009**, *390*, 109−114.
(4) Parkinson, G. N.; Lee, M. P.; Neidle, S. *Nature* **2002**, *417*, 876−880.
(5) Siddiqui-Jain, A.; Grand, C. L.; Bearss, D. J.; Hurley, L. H. *Proc. Natl. Acad. Sci. U. S. A.* **2002**, *99*, 11593−11598.
(6) Dexheimer, T. S.; Sun, D.; Hurley, L. H. *J. Am. Chem. Soc.* **2006**, *128*, 5404−5415.
(7) Morris, M. J.; Negishi, Y.; Pazsint, C.; Schonhoft, J. D.; Basu, S. *J. Am. Chem. Soc.* **2010**, *132*, 17831−17839.
(8) Balasubramanian, S.; Hurley, L. H.; Neidle, S. *Nat. Rev. Drug Discovery* **2011**, *10*, 261−275.
(9) Brooks, T. A.; Hurley, L. H. *Nat. Rev. Cancer* **2009**, *9*, 849−861.
(10) Ou, T. M.; Lu, Y. J.; Tan, J. H.; Huang, Z. S.; Wong, K. Y.; Gu, L. Q. *ChemMedChem* **2008**, *3*, 690−713.
(11) Neidle, S. *Curr. Opin. Struct. Biol.* **2009**, *19*, 239−250.
(12) Balasubramanian, S.; Neidle, S. *Curr. Opin. Chem. Biol.* **2009**, *13*, 345−353.
(13) Mathad, R. I.; Yang, D. *Methods Mol. Biol.* **2011**, *735*, 77−96.
(14) Davis, J. T. *Angew. Chem., Int. Ed.* **2004**, *43*, 668−698.
(15) Gonzalez, V.; Wilson, T.; Kurihara, I.; Imai, A.; Thomas, J. A.; Otsuki, J. *Chem. Commun.* **2008**, *16*, 1868−1870.
(16) Yang, P.; De Cian, A.; Teulade-Fichou, M. P.; Mergny, J. L.; Monchaud, D. *Angew. Chem., Int. Ed.* **2009**, *48*, 2188−2191.
(17) Meguellati, K.; Koripelly, G.; Ladame, S. *Angew. Chem., Int. Ed.* **2010**, *49*, 2738−2742.
(18) Xu, L.; Zhang, D.; Huang, J.; Deng, M.; Zhang, M.; Zhou, X. *Chem. Commun.* **2010**, *46*, 743−745.
(19) Jian, J. W.; Huang, C. C. *Chem.—Eur. J.* **2011**, *17*, 2374−2380.
(20) Yang, Q.; Xiang, J.; Yang, S.; Zhou, Q.; Li, Q.; Tang, Y.; Xu, G. *Chem. Commun.* **2009**, 1103−1105.
(21) Yang, Q.; Xiang, J. F.; Yang, S.; Li, Q.; Zhou, Q.; Guan, A.; Li, L.; Zhang, Y.; Zhang, X.; Zhang, H.; Tang, Y.; Xu, G. *Anal. Chem.* **2010**, *82*, 9135−9137.
(22) Yang, Q.; Xiang, J.; Yang, S.; Li, Q.; Zhou, Q.; Guan, A.; Zhang, X.; Zhang, H.; Tang, Y.; Xu, G. *Nucleic Acids Res.* **2010**, *38*, 1022−1033.
(23) Monchaud, D.; Allain, C.; Teulade-Fichou, M. P. *Nucleosides, Nucleotides Nucleic Acids* **2007**, *26*, 1585−1588.
(24) Menacher, F.; Rubner, M.; Berndl, S.; Wagenknecht, H. A. *J. Org. Chem.* **2008**, *73*, 4263−4266.
(25) Berndl, S.; Wagenknecht, H. A. *Angew. Chem., Int. Ed.* **2009**, *48*, 2418−2421.
(26) Lubitz, I.; Zikich, D.; Kotlyar, A. *Biochemistry* **2010**, *49*, 3567−3574.
(27) Lu, Y. J.; Yan, S. C.; Chan, F. Y.; Zou, L.; Chung, W. H.; Wong, W. L.; Qiu, B.; Sun, N.; Chan, P. H.; Huang, Z. S.; Gu, L. Q.; Wong, K. Y. *Chem. Commun.* **2011**, *47*, 4971−4973.
(28) Monchaud, D.; Allain, C.; Teulade-Fichou, M. P. *Bioorg. Med. Chem. Lett.* **2006**, *16*, 4842−4845.
(29) Largy, E.; Hamon, F.; Teulade-Fichou, M. P. *Anal. Bioanal. Chem.* **2011**, *400*, 3419−3427.
(30) Tan, J. H.; Ou, T. M.; Hou, J. Q.; Lu, Y. J.; Huang, S. L.; Luo, H. B.; Wu, J. Y.; Huang, Z. S.; Wong, K. Y.; Gu, L. Q. *J. Med. Chem.* **2009**, *52*, 2825−2835.
(31) Hou, J. Q.; Tan, J. H.; Wang, X. X.; Chen, S. B.; Huang, S. Y.; Yan, J. W.; Chen, S. H.; Ou, T. M.; Luo, H. B.; Li, D.; Gu, L. Q.; Huang, Z. S. *Org. Biomol. Chem.* **2011**, *9*, 6422−6436.
(32) Mishra, A.; Behera, R. K.; Behera, P. K.; Mishra, B. K.; Behera, G. B. *Chem. Rev.* **2000**, *100*, 1973−2012.
(33) West, W.; Pearce, S. *J. Phys. Chem.* **1965**, *69*, 1894−903.
(34) Rösch, U.; Yao, S.; Wortmann, R.; Würthner, F. *Angew. Chem., Int. Ed.* **2006**, *45*, 7026−7030.
(35) Phan, A. T.; Mergny, J. L. *Nucleic Acids Res.* **2002**, *30*, 4618−4625.
(36) Lin, S.; Li, S.; Chen, Z.; He, X.; Zhang, Y.; Xu, X.; Xu, M.; Yuan, G. *Bioorg. Med. Chem. Lett.* **2011**, *21*, 5987−5991.
(37) Membrino, A.; Cogoi, S.; Pedersen, E. B.; Xodo, L. E. *PLoS One* **2011**, *6*, e24421.
(38) Hounsou, C.; Guittat, L.; Monchaud, D.; Jourdan, M.; Saettel, N.; Mergny, J. L.; Teulade-Fichou, M. P. *ChemMedChem* **2007**, *2*, 655−666.
(39) Fedoroff, O. Y.; Salazar, M.; Han, H.; Chemeris, V. V.; Kerwin, S. M.; Hurley, L. H. *Biochemistry* **1998**, *37*, 12367−12374.
(40) Lu, Y. J.; Ou, T. M.; Tan, J. H.; Hou, J. Q.; Shao, W. Y.; Peng, D.; Sun, N.; Wang, X. D.; Wu, W. B.; Bu, X. Z.; Huang, Z. S.; Ma, D. L.; Wong, K. Y.; Gu, L. Q. *J. Med. Chem.* **2008**, *51*, 6381−6392.